

March 1973

LRP 61/73

SIMULATION OF BELT PINCH EXPERIMENTS INCLUDING
THE CIRCUIT EQUATIONS

D.W. Ignat and F. Hofmann

Centre de Recherches en Physique des Plasmas
ECOLE POLYTECHNIQUE FEDERALE DE LAUSANNE

SIMULATION OF BELT PINCH EXPERIMENTS INCLUDING
THE CIRCUIT EQUATIONS

D.W. Ignat and F. Hofmann

A b s t r a c t

An existing 1-D MHD code was modified to compute belt pinch experiments including the interaction between the plasma and the external circuit and self-consistent determination of the field in the toroidal core. Results of a computation simulating the Garching experiment are compared with those of a similar calculation which assumes a sine-wave time dependence for the current in the coil. Simulations of the belt pinch presently under construction at this laboratory were executed. Ion temperatures of ~ 200 eV with a 10 mTorr D_2 filling were computed.

Lausanne


Introduction

Computer codes which solve numerically one dimensional magneto-hydrodynamic equations have found wide application in the design and analysis of experiments in plasma physics. For example, the Hain-Roberts code¹ developed at Culham has been employed to show that the diffusion in the 8-meter theta pinch is anomalous at early times and classical after about 2μ seconds². During the past several years this laboratory has developed a one-dimensional MHD code for the simulation of the pinch experiments performed here. This code has served well in analysis of the rotating magnetic field pinch^{3,4}, the curved theta pinch, and the hot theta-pinch now being built to study the tenuous plasma remaining outside the dense core. Recent work has produced a hard core version. A simulation study of the belt pinch genre of experiments, and in particular the Garching Belt Pinch^{5,6}, has been published⁷. Until now the user had to supply the computation with the magnetic field at the boundaries as a function of time, even though one is not free to make such specification due to the requirements of self-consistency. Instead, one can specify only the various circuit parameters such as capacity and initial charge on the capacitor bank, stray inductance and resistance, and geometry of the conductors surrounding the plasma. The actual fields applied are a result of the interaction between the plasma and these parameters. Specification of fields implies the assumption that the errors incurred by doing so are not more serious than the other shortcomings of a one-dimensional MHD model.

In the case of the belt pinch^{5,6}, one can identify two reasons that this assumption may cause partially misleading results. First, belt pinches are inherently large devices with a large inductance which changes considerably with time. The rise of the current (and therefore

field) may not resemble a sine wave but can instead start rising extremely rapidly, reflecting only the stray inductance, and then slow down sharply as the plasma collapses and the load inductance moves to its full value. An actual experiment can be expected to exhibit a shorter collapse time and possibly a higher temperature than a prediction based on a field which climbs according to the average total inductance and bank parameters. Second, the poloidal field at the inner boundary depends on both the toroidal current in the coil windings and the poloidal field in the core of the torus. This field, in turn, depends on the location and magnitude of toroidal currents flowing in the plasma. Specification of the inner poloidal field is then doubly difficult, but one cannot guess easily at the sort of error made by such specification.

Motivated by the above two considerations, we have modified the computation to handle self-consistently the interaction between the plasma and the external circuit. Circuit parameters and coil geometry are now the only specified quantities, with the fields arising naturally. We have made investigations of the Garching Belt Pinch^{5,6} and the one under construction at this laboratory with the code as modified. For comparison, we have made one run on the Garching experiment in which the current in the circuit was forced to be a sine wave characteristic of the total average inductance, bank capacity and charging voltage. We find that in such a case, the plasma collapse time is slower and early temperatures are lower than in the more correct computation, as expected. The final plasma temperature in the sine wave case is higher, contrary to expectations. The fundamental reason appears to be that the assumption of a sine-shaped current implies the existence of tube voltages which can exceed the "bank voltage" by about 100 kV.



Coordinate System and Geometrical Parameters

We choose right cylindrical coordinates (r, θ, z) with the z -axis coincident with the major axis of the torus (See Fig. 1). In contrast with more common usage for toroidal problems, the z -direction is then poloidal and the θ -direction is toroidal. The plasma exists at r_p between the inner cylindrical surface (named "core") of the compression coil at r_c and the outer surface (named "wall") at r_w . Since we allow only r -variations in the calculation, the z -extent of the compression coil (H) and of the plasma play no role except in estimating the inductance of the system.

The toroidal field $B_\theta(r)$ results from the circuit current I flowing in the z -direction on the core surface. The return on the wall surface is in the negative z -direction. The poloidal field $B_z(r)$ arises from θ -components given to I by twisting the current channel into a helical shape. The helices are taken to be right-handed in the core and left-handed at the wall. We characterize the helix at the core (wall) by the angle α_c (α_w) made with the vertical. The pitch P and helical rotation Θ in the height H are related to the α 's by

$$P_{c,w} = \frac{2\pi r_{c,w}}{\tan \alpha_{c,w}} \quad \Theta_{c,w} = \frac{H \tan \alpha_{c,w}}{r_{c,w}}$$

The B_z caused by this configuration is positive inside the core, negative between the core and the plasma because the conducting plasma tries to conserve the flux initially inside it, and positive again between the plasma and the wall. Thus, poloidal flux encircles the plasma.

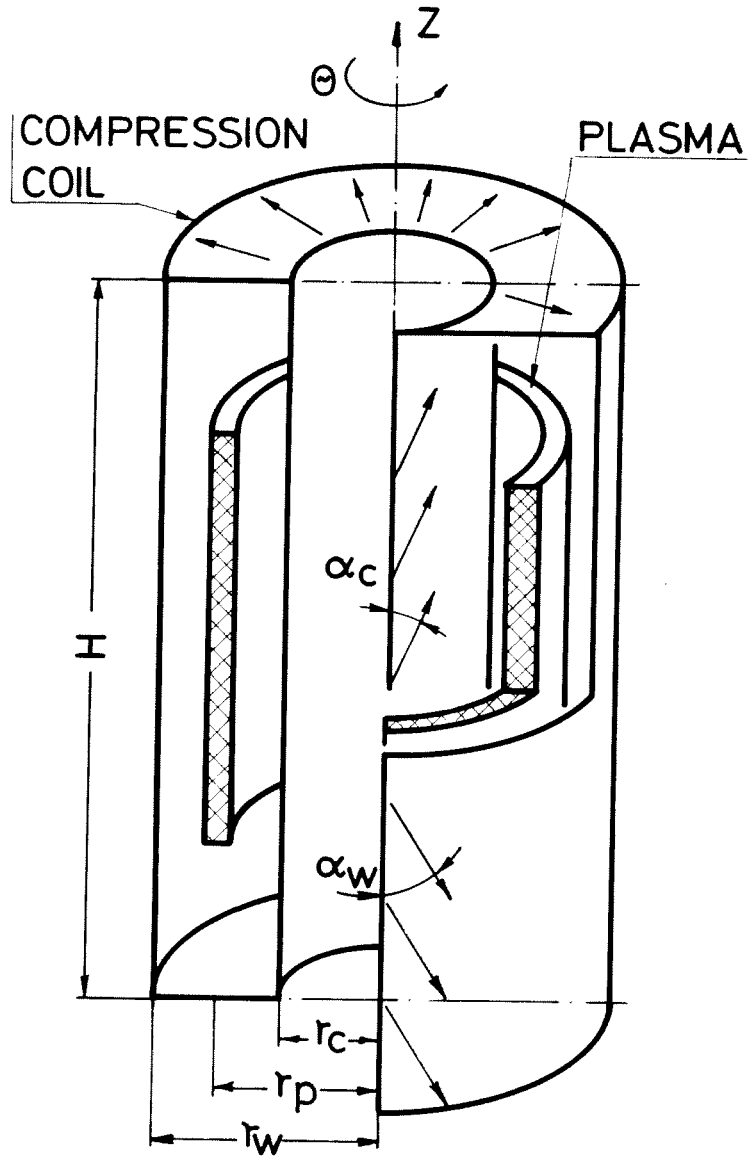


Fig. 1 Schematic, cut-away drawing of the belt pinch experiment. The arrows on the surface of the core ($r=r_c$), the wall ($r=r_w$) and the top annulus show the direction of \vec{c} current flow. The α_c and α_w angles characterize the helicity given to the current channel by twisting the conductors.

At the coil extremities, radial currents flow in annular disks in connecting the core and wall. These currents are ignored in the present analysis.

Simple Analysis

We begin by developing in a simple way the various important parameters and considerations for the belt pinch. This is done to give the reader a general idea of the experiment we are discussing which, with helical and toroidal shapes for current and field, is not easy to visualize.

In what follows, z-variations are ignored, and the plasma "radius" is a . That is, the thickness is $2a$. We assume the plasma excludes all B_z field and a portion of the B_θ field so that across a boundary B_θ changes by the factor $\sqrt{1 - \beta_\theta}$. The quantity β_θ is approximately the familiar β , and equals the kinetic pressure divided by the pressure associated with the vacuum B_θ field at the same radius in the limit of $|B_z / B_\theta|$ going to zero.

The fields, under the assumption that the conducting plasma holds the flux inside $(r_p - a)$ to zero, are:

In the core, $r < r_c$

$$B_\theta(r) = 0; \quad B_z(r) = \frac{\mu_0 I}{2\pi r_c} \tan \alpha_c \left[\frac{(r_p - a)^2 - r_c^2}{(r_p - a)^2} \right] \quad (1)$$

Between the core and plasma, $r_c < r < r_p - a$

$$B_\theta(r) = \frac{\mu_0 I}{2\pi r} \quad B_z(r) = -\frac{\mu_0 I}{2\pi r_c} \tan \alpha_c \left[\frac{r_c^2}{(r_p - a)^2} \right] \quad (2)$$

In plasma, $r_p - a < r < r_p + a$

$$B_{\theta}(r) = \frac{\mu_0 I}{2\pi r} \sqrt{1 - \beta_{\theta}} \quad B_z(r) = 0 \quad (3)$$

Between plasma and wall, $r_p + a < r < r_w$

$$B_{\theta}(r) = \frac{\mu_0 I}{2\pi r} \quad B_z(r) = \frac{\mu_0 I}{2\pi r_w} \tan \alpha_w \quad (4)$$

Outside the plasma radius the poloidal field is positive, and inside this radius B_z is negative. Thus poloidal field totally encircles the plasma. The toroidal field gets weaker with larger radius so the poloidal field must be bigger for $r > (r_p + a)$ than for $r < (r_p - a)$ in order to have a toroidal equilibrium. We quantify this idea by demanding pressure balance on both plasma surfaces and taking $(a/r_p) \ll 1$. Then

$$4\beta_{\theta} (a/r_p) + \frac{r_c^2}{r_p^2} \tan^2 \alpha_c = \frac{r_p^2}{r_w^2} \tan^2 \alpha_w \quad (5)$$

To avoid the kink instability the Kruskal limit must not be exceeded. To stay below the Kruskal limit, the toroidal pitch of field lines at the plasma surface must exceed the toroidal circumference of the plasma by a factor q_{\min} . Assuming ϵ to be a small positive quantity, we have

$$\frac{H B_{\theta}(r=r_p-a-\epsilon)}{|B_z(r < r_p-a)|} + H \frac{B_{\theta}(r=r_p+a+\epsilon)}{|B_z(r > r_p+a)|} > q_{\min} \frac{2\pi r_p}{r_p} \quad (6)$$

$$q_{\min} = \frac{2}{2 - \beta_{\theta}}$$

More specifically, with $a \rightarrow 0$, and $\beta_\theta = 1$ the above yields:

$$H \left(\frac{r_p}{r_c \tan \alpha_c} + \frac{r_w}{r_p \tan \alpha_w} \right) > 2(2\pi r_p) \quad (7)$$

In Eq.(7), we see the primary motivation for belt pinch experiments: H can be made as large as one pleases independently of other parameters to avoid the Kruskal-Shafranov kink mode.

We now wish to compute the inductance, and do so from the total flux Ψ enclosed in following the current path around the circuit and using $L = \Psi/I$. Again we take $a \rightarrow 0$. The total flux is the sum of the B_θ flux enclosed inside the toroidal winding $\int_{r_c}^{r_w} B_\theta(r) H dr$, plus the B_z flux in the core $B_z(r < r_c) \pi r_c^2$ multiplied by the number of times the core is encircled by the current path $H \tan \alpha_c / (2\pi r_c)$, plus the total flux inside the wall $B_z(r > r_p) \pi (r_w^2 - r_p^2)$ multiplied by the number of times this flux is encircled $H \tan \alpha_w / (2\pi r_w)$. The inductance is then

$$L = \frac{\mu_0 H}{4\pi} \left\{ 2 \ln(r_w/r_c) + \tan^2 \alpha_c \left(\frac{r_p^2 - r_c^2}{r_p^2} \right) + \tan^2 \alpha_w \left(\frac{r_w^2 - r_p^2}{r_w^2} \right) \right\} \quad (8)$$

Method of Solution

In making the MHD computation consistent with the circuit equations, there are two problems. First, one must find the current flowing in the coil from consideration of inductance. Second, one must find the proper B_z in the core.

Clearly these problems are coupled because the inductance depends on the field in the core and vice-versa. We note from Eq.(8), however, that the contribution to inductance made by the core is small compared with that made by the θ -field. Therefore, we treat the problems independently.

The circuit equations are:

$$V(t) = R_0 I(t) + L_0 \frac{dI(t)}{dt} + \frac{d\psi(t)}{dt} \quad (9)$$

$$\frac{dV(t)}{dt} = -I(t)/C \quad (10)$$

where

- $V(t)$ = voltage on capacitor bank
- $I(t)$ = current flowing from bank to coil
- R_0 = parasitic resistance
- L_0 = parasitic inductance
- $\psi(t)$ = flux linked by coil as computed as in arriving at Eq.(8)

In the MHD simulation ψ is found at the end of each time step by integration over the spatial mesh. The time derivative of this quantity is badly behaved, especially for small time steps, because of small fluctuations in the integral due to the coarse spatial mesh and the division by a small quantity. Therefore we deal with ψ by integrating this equation formally. Defining $\xi(t) = \int_0^t (V(t) - I(t)R_0)dt$ the difference equations become

$$I_{n+1} = \left\{ \xi_n + \frac{(t_{n+1}-t_n)}{2} \left[V_{n+1} + V_n + R_0(I_n + I_{n+1}) \right] - \psi_{n+1} \right\} / L_0 \quad (11)$$

11

$$V_{n+1} = V_n - \left(\frac{I_{n+1} + I_n}{2} \right) \left(\frac{t_{n+1} - t_n}{c} \right) \quad (12)$$

Here t represents time and the subscripts $(n + 1)$ and (n) denote the new and old values of quantities. To solve this system, one must iterate on φ_{n+1} through the MHD solution. This would consume computing time prohibitively, so φ_{n+1} was simply guessed according to

$$(\varphi_{n+1})_{\text{guessed}} = \varphi_n + \frac{(\varphi_n - \varphi_{n-1})}{(t_n - t_{n-1})} (t_{n+1} - t_n) \quad (13)$$

Then after solution for $(I, V)_{n+1}$, the plasma physics was run and the resultant φ_{n+1} computed. We formed a figure of merit for the guess,

$$F_\varphi = \left| \frac{(\varphi_{n+1} - (\varphi_{n+1})_{\text{guessed}})}{\varphi_{n+1}} \right| \left(\frac{1 \mu\text{sec}}{(t_{n+1} - t_n)} \right) \quad (14)$$

which is roughly the relative error per microsecond of plasma evolution. If F_φ was large no attempt at correction was made. In fact F_φ was almost always less than 0.01 except near $t = 0$ when φ is near zero. At these early times the inductance of the plasma influences weakly the current flowing in the circuit. In principle, Faraday's law can be used to determine the poloidal field in the core (B_{core}). From the currents flowing in the plasma and the resistivity, one can find $E_\theta(r)$ and this can be related to B_{core} by

$$-2\pi r E_\theta(r) = \pi r_c^2 \frac{dB_{\text{core}}}{dt} + \frac{d}{dt} \int_{r_c}^r B_z(r) 2\pi r' dr'$$

In practice, this procedure caused difficulty because the $E_\theta(r)$ values, being derived quantities, were not sufficiently consistent as time

12

advanced. We avoided the problem by assuming that $E_{\theta} = 0$ for all time at the center of the plasma which was defined as the point where $B_z(r)$ crossed zero. This meant the plasma constrained the total z -flux inside its center to be zero. The Garching group has observed this behavior experimentally⁸. At the end of each time step we computed the flux between r_c and the plasma center, and then forced $\pi r_c^2 B_{core}$ to be equal and opposite. For the next time step a guess at B_{core} was made:

$$(B_{core\ n+1})_{\text{guessed}} = B_{core\ n} + \frac{(B_{core\ n} - B_{core\ n-1})}{(t_n - t_{n-1})} (t_{n+1} - t_n)$$

and the boundary condition on $B_z(r = r_c)$ resulted from this guess and the current I_{n+1} flowing in the coil. After the time step we formed a figure of merit for the guess analogous to that of Eq.(14). This quantity behaved similarly to F_{ψ} .

The stability of our scheme was tested by making one run in which the guessed quantities were identical to the values at the end of the last time step, i.e., the time derivatives were assumed zero in making a guess.

Perceptible but unimportant differences occurred in all resulting quantities. The difference can be well described as a small time-lag in the development of the pinch. This result and the good behavior of our figures of merit makes us confident that our solutions are appropriate. This method could be applied to any future simulation of other kinds of experiments with straightforward application of the procedure outlined here, provided the external circuit can be modeled accurately with equations like (9) and (10).

Simulation of Garching Experiment

Table I summarizes all the parameters assumed in the computation.

T a b l e I

Parameters of the Garching Belt-Pinch Assumed in the Computation

r_c	15 cm	$V(t=0)$	40 kV
r_w	31 cm	filling pressure	50 mTorr D_2
H	100 cm	initial % ionization	20 %
$\tan\alpha_c$.424	initial temperature	$T_1 = T_e = 1eV$
$\tan\alpha_w$.604	resistivity	classical
C	150 μ Farad		
R_o	.001 ohm		
L_o	25 n henry		

Where possible, these numbers have been taken from published data; otherwise, reasonable guesses have been made. In table II we give a summary of the resultant parameters of general interest. The β_θ value listed is very approximate because the plasma continued to bounce strongly for the duration of our calculation. Thus a determination under static conditions was not possible.

T a b l e II

Computed Results for the Garching Experiment

Time of zero bank voltage	8.479 μ sec
Maximum current	1.05 MA
Resultant B_θ (r=23 cm)	10 kG
Max. mean Temp (at about 5 μ s)	8.5 eV
Max. peak density	$4 \times 10^{16} \text{ cm}^{-3}$
β_θ	~.5
Collapse time	1.95 μ s
Plasma inductance after collapse	165 nH

We will now examine how the interaction between the plasma and the circuit proceeded. In Fig. 2 we graph the thermal energies of electrons and ions averaged over all particles, the inductance of the tube as defined by the total magnetic flux enclosed by the external circuit divided by the current flowing therein, the current in the coil, and the voltages across the capacitor bank and the tube.

At very early times we see the current rising extremely fast since only the small stray inductance of 25 nH is present to limit the rise. The plasma temperatures also rise quickly reflecting the shape of the field rise. At about $1/2 \mu\text{s}$, however, the coil voltage has risen to very near the bank voltage and the current increase proceeds much more slowly. The temperature rise levels off also. As the imploding plasma reaches maximum compression, the temperature doubles because of adiabatic compression and again falls quickly as the plasma expands. As soon as the plasma motion reverses the tube voltage falls and the current rises sharply with a rate of change almost equal to that of time zero. Now the cause of the sharp rise is the plasma working on the field rather than the initial low inductance in the circuit. The process continues with plasma size, temperature, and inductance bouncing and causing oscillations in the circuit. Notice that on all bounces after the first, the tube voltage actually goes above the bank voltage and the current shows a sharp drop.

It is natural to wonder how the general results of the calculation, as given in Table II, would differ if we ignored the circuit equations and assumed that the current rose as a sine wave. We have carried out such a calculation by ignoring ψ in Eq.(9) and setting L_0 to 190 nH. General results are summarized in Table III. As one expects, the plasma collapse time is later. The relative change is significant at 25 %.

T a b l e I I I
Computed Results for the Garching Experiment
with Circuit Equations Ignored

Time of zero Bank Voltage current	8.462 μ sec
Max Current	1.1 MA
Resultant B_{θ} (r=23 cm) (vacuum field)	10 kG
Maximum mean Temp(at 5 μ s)	9.4 eV
Max peak density	$3.8 * 10^{16} \text{ cm}^{-3}$
β_{θ}	~.5
Collapse time	2.45 μ s

There is a noticeable but less significant change in the maximum average temperature, which has increased by 10 % from 8.5 to 9.4 eV. The development of the calculation is shown in Fig. 3. Here we can see the qualitative reason for the increased temperature. The tube voltage, which of course was ignored in the computation since the circuit equations were inoperative, experienced excursions about the bank voltage of over one hundred kilovolts. The power being applied, which is the product of the sine wave current and this voltage then also experienced excursions, and those were predominantly positive. Thus, after about 2 μ s the net energy delivered to the plasma coil in this case exceeds that delivered in the computation which included the circuit equations.

The efficiency of energy transfer from the field to the plasma is greater for the simulation which includes circuit equations, however. For example, at the first plasma collapse the transfer is 18 % and 13 % efficient for the realistic calculation and the calculation which imposes sine-wave shape for the current, respectively. The two effects work against each other so the resultant temperatures are not much different.

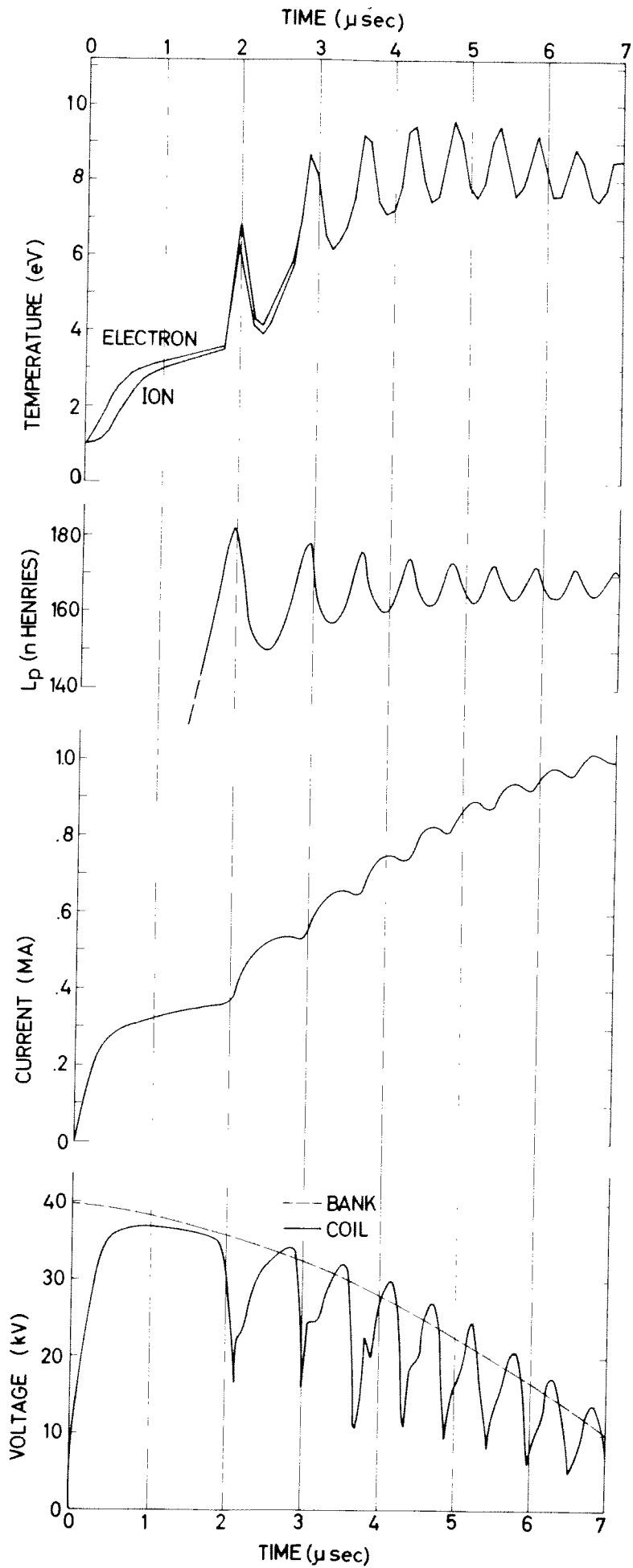


Fig. 2 Computed time development of the Garching belt pinch experiment as represented by four parameters. The filling pressure assumed is 50 mTorr D_2 .

17

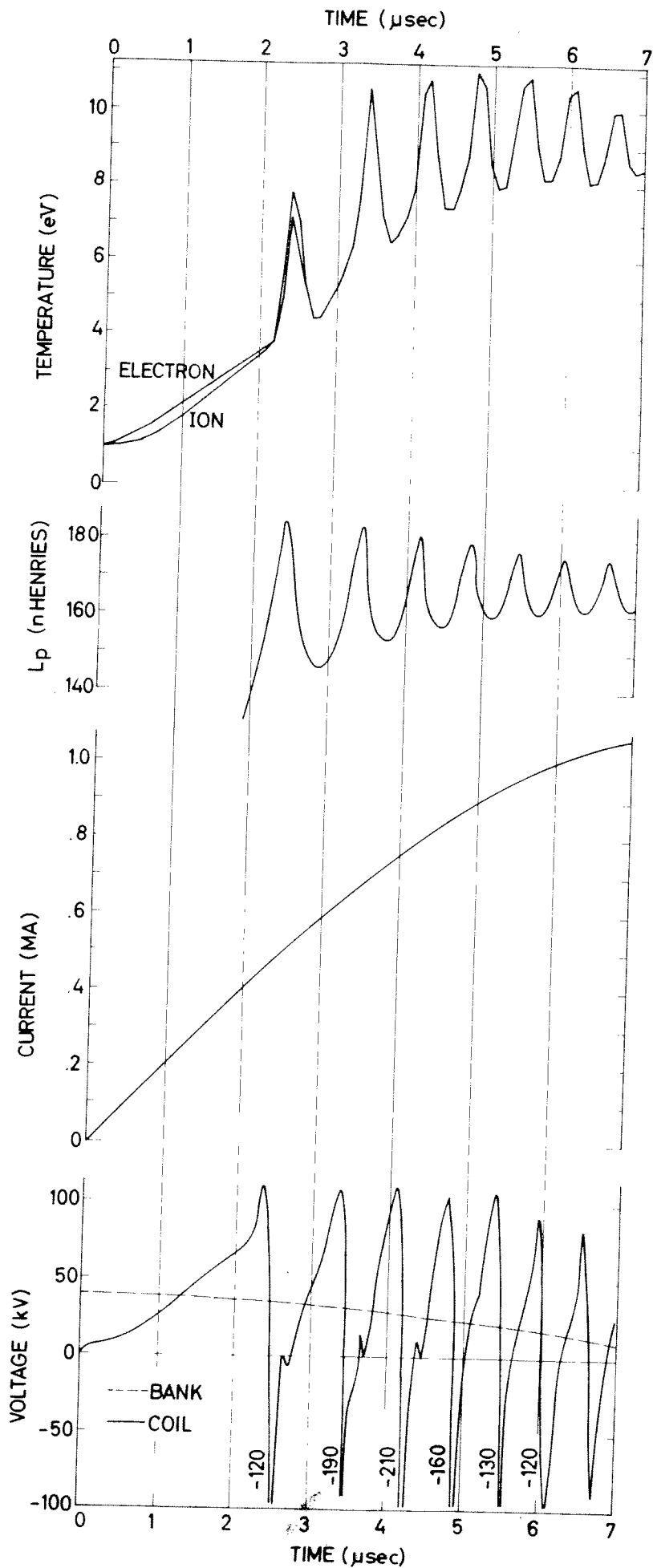


Fig. 3 Computed time development of the Garching belt pinch experiment as in Fig. 2 but under the assumption that the current is a sine wave.

Simulation of the CRPP Belt Pinch

We have made two simulations of the belt pinch under construction at this laboratory. The circuit-plasma interaction is included. Since the compression coil is fed at two places in order to get twice the bank voltage around the coil, some straightforward modifications were required in the equations used. (The flux linked in going around the coil was halved, and in calculating the fields the total current flowing through the bank was divided by 2).

Table IV gives the important parameters.

T a b l e IV
Assumed Parameters for the CRPP Belt-Pinch

r_c	10.5 cm	$V(t=0)$	40 kV
r_w	21.4 cm	filling pressure	20, 10 mTorr D_2
H	65.0 cm	initial % ionization	20 %
$\tan\alpha_c$	0.444	initial temperatures	$T_e = T_i = 1eV$
$\tan\alpha_w$	0.647	resistivity	classical
C	150 μ Farad		
R_o	0.001		
L_o	20 n henry		

T a b l e V
Summary of Computed Results for the CRPP Belt Pinch

<u>PARAMETER</u>	<u>p = 20 mTorr D₂</u>	<u>p = 10 mTorr D₂</u>
Time of zero bank voltage	4.45 μs	4.42 μs
Maximum current	2.04 MA	2.04 MA
Resultant B _θ (r=16 cm)	12.5 kG	12.5 kG
Average ion (electron) temperature at 3.5 μs	32 eV(32 eV)	213 eV(81 eV)
Max n _e at 3.5 μs	1.58 * 10 ¹⁶ cm ⁻³	.613 * 10 ¹⁶ cm ⁻³
β _θ at 3.5 μs	.26	.47
Collapse time	.91 μs	.71 μs
Plasma inductance after collapse	33.5 nH	31 nH

The higher temperatures here are due to the lower filling pressures assumed and the faster rise time of the magnetic field. The evolution of the two pinches is shown in Fig. 4 and Fig. 5. We emphasize the fact that the hotter pinch exhibits much less bouncing than the colder one. This is due to the increased viscosity for the higher temperatures.

In fact, it appears that proper inclusion of the circuit interaction may be unnecessary if the pinch is really going to be hot. Self-consistent determination of the poloidal field in the core as we have done here is desirable in any case, however, since this will influence the equilibrium position of the plasma.

Finally, Fig. (6) shows the field and density distribution at 3.5 μsec for the 10 mTorr D₂ filling pressure.

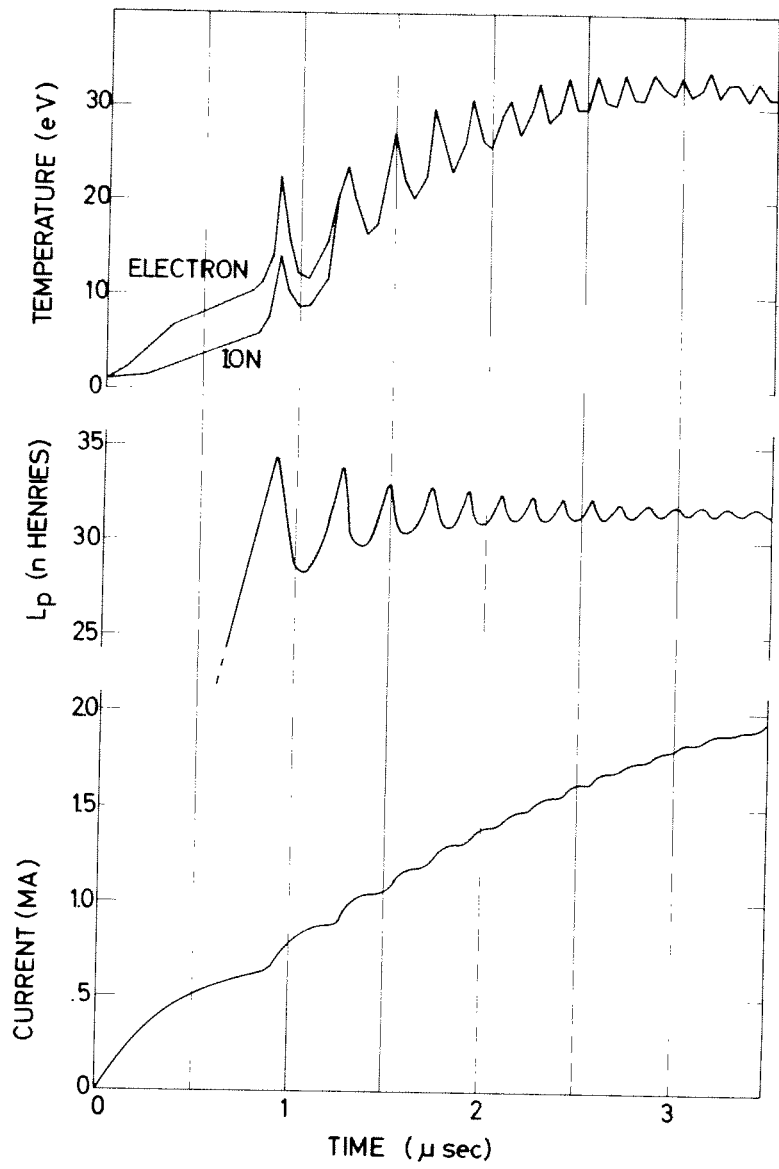


Fig. 4 Time development of temperature, plasma inductance and current from the capacitor bank as computed for the belt pinch of the CRPP assuming a filling pressure of 20 mTorr D_2 .

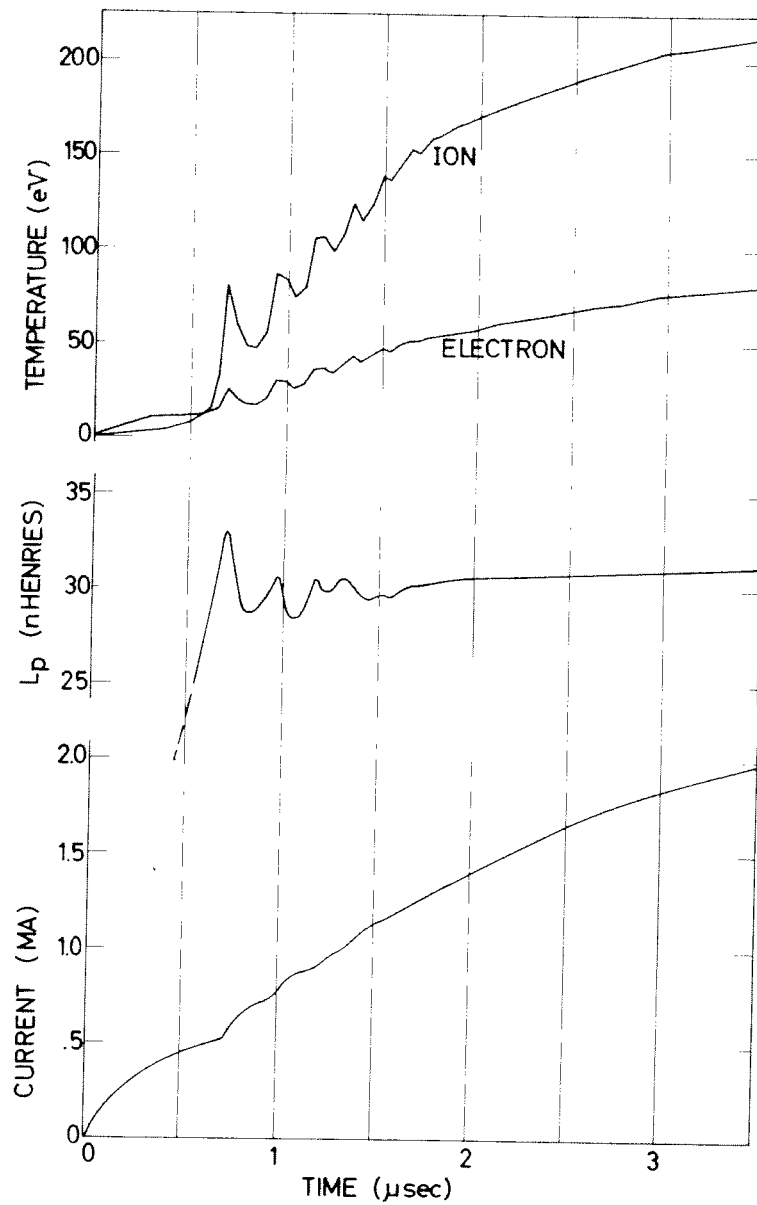


Fig. 5 Time development of temperature, plasma inductance and current from the capacitor bank as computed for the belt pinch of the CRPP assuming a filling pressure of 10 mTorr D_2 .

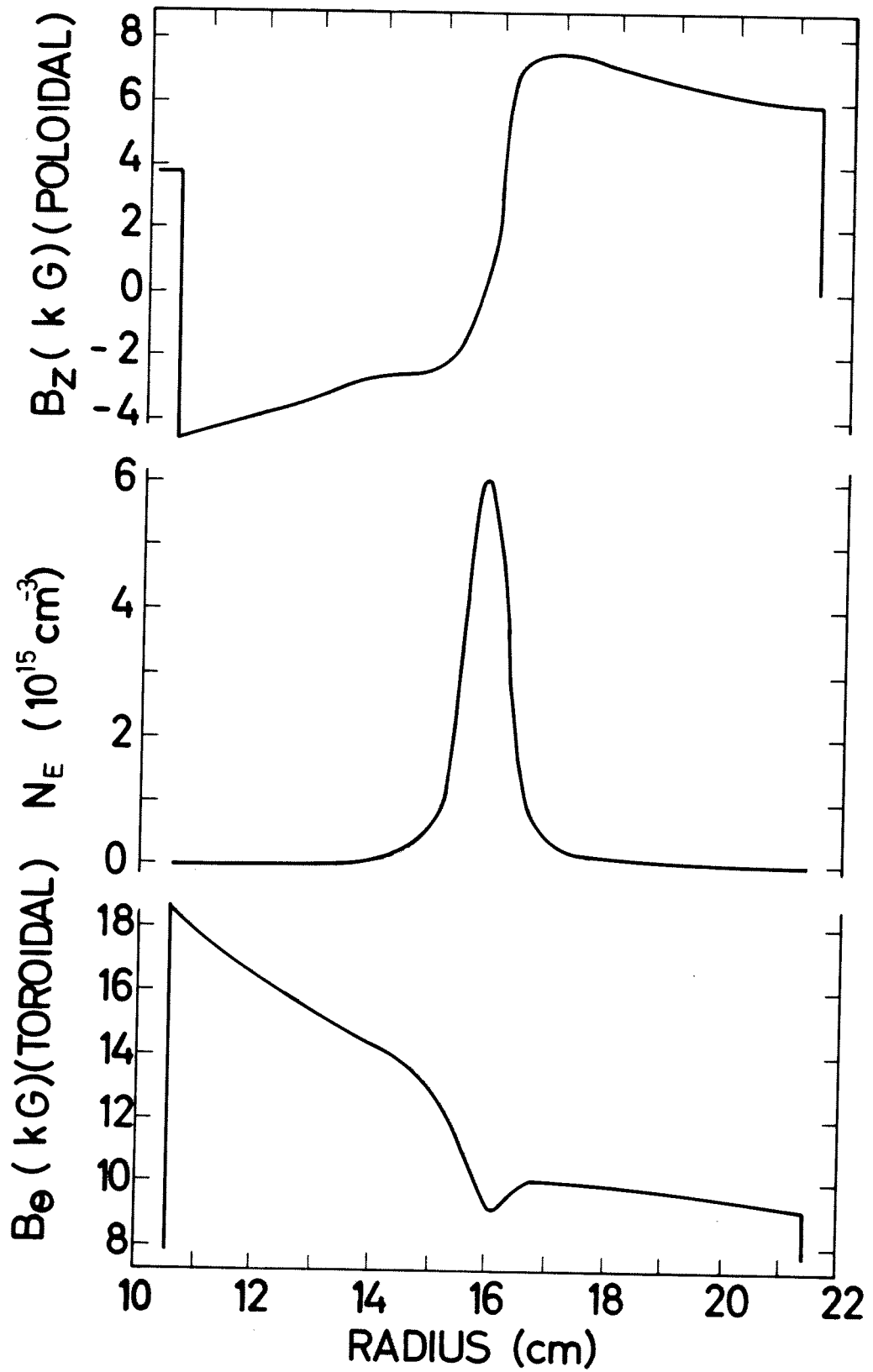


Fig. 6 Field and density profiles computed for the belt pinch of the CRPP at $3.5 \mu\text{s}$ after firing the capacitor bank assuming a filling pressure of 10 mTorr D_2 .

Conclusion

We have successfully modified the Lausanne 1-D MHD code to include the interaction between plasma and external circuit and to determine self-consistently (in a high-conductivity approximation) the poloidal field in the core of the torus. The method of solving this problem is stable, and the accuracy is of the order of 1 % based on our figure of merit. Therefore, the method should be at least as accurate as the rest of the model. The basic method can be applied to simulations of other experiments. We have simulated the Garching belt pinch and have found temperature near 10 eV for filling pressure of 50 mTorr D_2 . We determined that one can expect proper inclusion of the circuit equations to decrease the collapse time and also decrease the temperature with respect to computations ignoring the circuit interaction. Finally, we have simulated the CRPP pinch and found $T_i \approx 200$ eV with a 10 mTorr D_2 filling.

Acknowledgment

Several head-clearing discussions with F. Troyon are gratefully acknowledged. This work was supported by the Fonds National Suisse de la Recherche Scientifique.

24

R e f e r e n c e s

1. HAIN K., HAIN G., ROBERTS K.V., ROBERTS S.J. and KOEPPENDOERFER W.,
Z. Naturf. 15a (1960) 1039.
2. BODIN H.A.B. and NEWTON A.A., Phys. Fluids 12 (1969) 2175.
3. HOFMANN F., Plasma Physics and Controlled Nuclear Fusion Research,
Volume I (1971) 267. International Atomic Energy Agency,
Vienna.
4. IGNAT D.W., HEYM A., HOFMANN F. and LIETTI A., Plasma Phys. (1973)
to be published.
5. WILHELM R. and ZWICKER H., Plasma Physics and Controlled Nuclear
Fusion Research, Volume I (1971) 259. International Atomic
Energy Agency, Vienna.
6. ZWICKER H. and WILHELM R., Fifth European Conference on Controlled
Fusion and Plasma Physics, Volume II (1972) 59.
7. HOFMANN F., Nuclear Fusion 13 (1973) to be published.
8. ZWICKER H., private communication.